Embedded-atom-method functions for the fcc metals Cu, Ag, Au, Ni, Pd, Pt, and their alloys

S. M. Foiles, M. I. Baskes, and M. S. Daw
Sandia National Laboratories, Livermore, California 94550
(Received 13 January 1986)

A consistent set of embedding functions and pair interactions for use with the embedded-atom method [M.S. Daw and M. I. Baskes, Phys. Rev. B 29, 6443 (1984)] have been determined empirically to describe the fcc metals Cu, Ag, Au, Ni, Pd, and Pt as well as alloys containing these metals. The functions are determined empirically by fitting to the sublimation energy, equilibrium lattice constant, elastic constants, and vacancy-formation energies of the pure metals and the heats of solution of the binary alloys. The validity of the functions is tested by computing a wide range of properties: the formation volume and migration energy of vacancies, the formation energy, formation volume, and migration energy of divacancies and self-interstitials, the surface energy and geometries of the low-index surfaces of the pure metals, and the segregation energy of substitutional impurities to (100) surfaces.

I. INTRODUCTION

Many problems in solid-state physics and materials science require a detailed understanding of the energetics and structure of nonuniformities in metals and alloys. Due to the lower symmetry and long-range strains generally found around defects and surfaces, the study of these problems requires techniques that can handle a large number of atoms. This, in turn, requires a model of a solid which is both accurate and computationally simple. Historically, these problems have been addressed with various pair-potential models of the energetics of the constituents of the solid.[1-3] This approach is certainly useful in many circumstances. However, there are some significant problems associated with the application of the pair potentials when the local environment is substantially different from the uniform bulk. This includes such problems as surfaces, grain boundaries, internal voids, and fracture processes.

Daw and Baskes[4,5] have proposed an alternative to the pair-potential approach based on density-functional ideas, which they call the embedded-atom method (EAM). As with pair-potential models, the energetics of an arbitrary arrangement of atoms can be calculated quickly, but the ambiguity of the volume dependence inherent in pair-potential models[6] is avoided. This new method has already been applied to several problems with good results. The applications to bulk pure metals include phonon spectra,[7] structure of liquid metals,[8] dislocation propagation,[9] and fracture properties.[4,5] It has been applied to surfaces and shown to provide realistic values for both the surface energies and geometries[5] including the prediction of the (1×2) surface reconstruction of Pt(110).[10] Furthermore, this approach has been applied successfully to segregation phenomena in Ni-Cu alloys.[11] The EAM has also been used to study hydrogen interactions with metals. It has predicted the ordered structures and critical temperatures of hydrogen adsorbed on Pd(111) (Ref. 12) and the influence of hydrogen on dislocation motion[9] and fracture.[4,5] Because the EAM provides a more realistic description of the metallic cohesion, it appears to be a desirable alternative to pair-interaction models.

As will be discussed below, in the EAM, the energy of each atom is computed from the energy needed to embed the atom in the local-electron density as provided by the other atoms of the metal. This electron density is approximated by the superposition of atomic-electron densities. Since this density is well defined at surfaces and in alloys, there are no ambiguities involved in this approach. Computationally, the EAM energy can be evaluated with about the same amount of work as simple pair potentials. Therefore, it is still feasible to perform large-scale computer simulations of a wide variety of phenomena. Thus the EAM provides a powerful new technique for atomistic calculations of metallic systems.

The purpose of this paper is to present a consistent set of embedding functions and short-range repulsive pair interactions which are suitable to describe the fcc metals Cu, Ag, Au, Ni, Pd, and Pt as well as all the alloy combinations of these elements. (While the parametric form for these functions may not be the only or best possible choice for a specific metal or alloy system, it is useful to have a common set of functions that provide a good description of a large set of metals and alloys. This facilitates the determination of trends over a range of metals or alloys.) These functions have been determined empirically by fitting the predicted results to the equilibrium density, sublimation energy, elastic constants, and vacancy-formation energy of the pure metals as well as to the heats of solution of the binary alloys.

The validity of these EAM functions will then be tested by calculating several properties of both the pure metals and the binary alloys. For the pure metals, the parametrization used here forces the lattice constant, sublimation energy, and bulk modulus to be exactly reproduced, as will be discussed below. As tests, the migration energies and formation volumes of vacancies and the formation energy, formation volume, and migration energy of divacancies and self-interstitials are computed and compared with the available experimental data. Also, the surface

energies and relaxed, but unreconstructed, surface geometries of the low-index faces of the pure metals are determined. For the alloys, the dilute limit of the segregation energy to (100) surface is computed for all the binary alloys.

II. THEORY

Within the framework of density-functional theory, the total electronic energy for an arbitrary arrangement of nuclei can be written as a unique functional of the total-electron density. The starting point of the EAM is the observation that the total-electron density in a metal is reasonably approximated by the linear superposition of contributions from the individual atoms. The electron density in the vicinity of each atom can then be expressed as a sum of the density contributed by the atom in question plus the electron density from all the surrounding atoms. This latter contribution to the electron density is a slowly varying function of position. By making the simplification that this background electron density is a constant, the energy of this atom is the energy associated with the electron density of the atom plus the constant background density. This defines an embedding energy as a function of the background electron density and the atomic species. In addition, there is an electrostatic energy contribution due to core-core overlap. These ideas have been developed by Daw and Baskes[5] and Daw,[13] who show that these ideas lead to an approximation for the total energy of the form

$$E_{\rm tot}=\sum_i F_i(\rho_{h,i})+\tfrac{1}{2}\sum_i\sum_{j\,(\neq i)}\phi_{ij}(R_{ij})\ . \tag{1}$$

In this expression, $\rho_{h,i}$ is the host electron density at atom i due to the remaining atoms of the system, $F_i(\rho)$ is the energy to embed atom i into the background electron density ρ, and $\phi_{ij}(R_{ij})$ is the core-core pair repulsion between atoms i and j separated by the distance R_{ij}. (Note that F_i only depends on the element of atom i and ϕ_{ij} only depends on the elements of atoms i and j.) The electron density is, as stated above, approximated by the superposition of atomic densities,

$$\rho_{h,i}=\sum_{j\,(\neq i)}\rho_j^a(R_{ij})\ , \tag{2}$$

where $\rho_j^a(R)$ is the electron density contributed by atom j. With this approximation for the electron density, the actual computations using this method do not require significantly more work than the use of pair-interaction models. Note that the embedding function $F_i(\rho)$ is universal, in that it does not depend on the source of the background electron density. Thus the same embedding function is used to calculate the energy of an atom in an alloy that is used in the pure material. This universality makes the EAM particularly appealing for studies of alloys.

To apply this method, the embedding functions, pair repulsions, and atomic densities must be known. The atomic densities will be taken from Hartree-Fock calculations[14,15] as discussed below. Approximate values of the embedding functions and pair interactions can be calculated from the formal definitions of these quantities within the density-functional framework as described by Daw.[13] These functions, however, only give qualitatively correct predictions of the material properties, so it is necessary to determine these functions empirically in order to obtain an accurate description. The first-principles calculations do give the following important information about the general behavior of these functions. The embedding energy (defined relative to the free-atom energy) must go to zero for zero electron density and should have a negative slope and positive curvature for the background electron densities found in metals. The pair-interaction term $\phi(R)$ is purely repulsive. This analysis also shows that the pair interaction between two different species can be approximated by the geometric mean of the pair interaction for the individual species. This observation, along with the Coulombic origin of the pair-interaction term, suggest writing the pair interaction between atoms of types A and B in terms of effective charges as

$$\phi_{AB}(R)=Z_A(R)Z_B(R)/R\ . \tag{3}$$

The effective charge is constrained to be positive and to decrease monotonically with increasing separation.

Daw and Baskes[5] showed that it is possible to empirically obtain embedding energies $F(\rho)$ and effective charges $Z(R)$ that accurately describe the energetics of pure Ni and Pd. They assumed functional forms for $F(\rho)$ and $Z(R)$ which meet the general conditions described in the preceding paragraph and adjusted the parameters to fit known bulk properties. In particular, they fit to the sublimation energy, lattice constant, elastic constants, vacancy-formation energy, and internal energy of the bcc phase. They also obtained functions for hydrogen and helium. These functions cannot be used to study alloys, though. The information used in their empirical fits actually only determines $F(\rho)$ and its first two derivatives for electron densities near the average host electron density $\rho_{\rm eq}$ of the bulk pure materials at equilibrium. While this provides sufficient information about $F(\rho)$ to perform many calculations for pure materials, the atoms in an alloy are embedded in electron densities substantially different from that in the pure material. In a subsequent paper, Foiles[11] showed that the zero-pressure equation of state of the pure material could be used to determine the embedding energy, $F(\rho)$ for a larger range of electron densities. This procedure was then applied to the Ni-Cu alloy system where it was used to investigate surface-segregation phenomena. The main objective of this work is to apply this same procedure to obtain a consistent set of embedding functions and pair interactions for the fcc metals Cu, Ag, Au, Ni, Pd, and Pt.

The information about $F(\rho)$ for densities well away from $\rho_{\rm eq}$ is obtained through the equation of state of the expanded or compressed metals for which the electron density at each lattice site is substantially different from $\rho_{\rm eq}$. Rose *et al.*[16] have shown that the sublimation energy of most metals as a function of lattice constant can be scaled to a simple universal function,

$$E(a)=-E_{\rm sub}(1+a^*)e^{-a^*}\ . \tag{4}$$

In this expression, $E_{\rm sub}$ is the absolute value of the sublimation energy at zero temperature and pressure. The

quantity a^* is a measure of the deviation from the equilibrium lattice constant,

$$a^*=(a/a_0-1)/(E_{\rm sub}/9B\Omega)^{1/2} . \quad (5)$$

Here, B is the bulk modulus of the material, a is a length scale characteristic of the condensed phase, which we will take to be the fcc lattice constant, a_0 is the equilibrium lattice constant, and Ω is the equilibrium volume per atom. This expression has been shown to given a good fit to the equation of state of numerous metals over a wide range of both expansion and compression. Further, the only input data needed are the equilibrium density, sublimation energy, and bulk modulus of the material, which are generally readily available.

Note that if the atomic electron densities $\rho_j^a(R)$ and the pair interaction $\phi(R)$ are both known, then the embedding energy can be uniquely defined by requiring the total energy of the homogeneous fcc solid, computed using Eq. (1) to agree with the universal equation of state given by Eq. (4). The problem then, is to determine the atomic electron densities and pair interactions.

The atomic electron density is assumed to be well represented by the spherically averaged free-atom densities calculated from Hartree-Fock theory by Clementi and Roetti[14] and McLean and McLean.[15] There is one ambiguity in using these atomic densities for the bulk. While the optimum electronic configuration is known for the free atom, it is not clear that this configuration will be the best representation of the electron density in the solid. For a pure material, this is not a serious problem. The main effect of changing the relative number of s and d electrons is to simply change the electron density for the distances that are actually used in these calculations by a multiplicative factor. This reflects the fact that the d-electron wave functions are quite small at the nearest-neighbor distance. Changing the atomic density by a constant factor, though, does not change the properties computed for a single element, because this change simply results in a rescaling of the argument of the embedding function as determined above. For a multicomponent system, however, changing the atomic density used for one of the components will strongly affect the mixing energies of the alloy. Thus it is essential for the alloy systems that a consistent choice be made for the electronic configurations assumed for the different metals.

The atomic densities in this work are computed from the Hartree-Fock wave functions by

$$\rho^a(R)=n_s\rho_s(R)+n_d\rho_d(R) , \quad (6)$$

where n_s and n_d are the number of outer s and d electrons and ρ_s and ρ_d are the densities associated with the s and d wave functions. (There are wave functions available for different atomic configurations, i.e., different occupations of the s and d orbitals. The configurations used in the current calculations are indicated in Table I. They have the number of s electrons closest to the values of n_s that are determined here in the manner discussed below.) The total number of s and d electrons, n_s+n_d, is fixed to be 10 for Ni, Pd, and Pt, and 11 for Cu, Ag, and Au. Thus the atomic density of each species depends on the single parameter, n_s. As will be discussed below, this parameter will be determined so as to give the proper heats of solution of the alloys.

The last quantity that is needed is the pair-repulsion term. In this work, we assume a simple parametrized form for $Z(R)$:

$$Z(R)=Z_0(1+\beta R^\nu)e^{-\alpha R} . \quad (7)$$

The pair interaction $\phi(R)$ is related to $Z(R)$ by Eq. (3). The value of Z_0 will be assumed to be given by the number of outer electrons of the atom, i.e., $Z_0=10$ for Ni, Pd, and Pt, while $Z_0=11$ for Cu, Ag, and Au. Thus there remain three parameters, α, β, and ν, to be determined. Empirically, it was found that the choice $\nu=1$ leads to a good representation of the elastic constants for Ni, Pd, and Pt, while $\nu=2$ worked better for Cu, Ag, and Au.

With the above assumptions, there are three adjustable parameters, α, β, and n_s, needed to determine the pair potential, atomic electron density, and embedding function for each material. These have been determined for the elements Cu, Ag, Au, Ni, Pd, and Pt so as to yield the elastic constants and vacancy-formation energy of each material as well as the dilute limits of the heats of solution of the binary alloys (when such information is available). Note that, due to the definition of the embedding function in terms of the equation of state of the pure materials, the equilibrium lattice constant, sublimation energy, and bulk modulus are guaranteed to be correct for the pure materials. The values of α and β are primarily determined by both the shear moduli of the pure materials and the vacancy-formation energy. The relative values of n_s are primarily determined by the heats of mixing of the alloys. Since n_s is primarily determined by the heats of alloying, there is an overall scale factor for the set of values for n_s which is undetermined by the fitting. The n_s for Cu is therefore arbitrarily chosen to be 1. Note that for this parametrization, there are 17 free parameters to be adjusted. The data for each pure metal provides three

TABLE I. Parameters defining the effective charges for the pair interactions [Eq. (7)] and atomic electron density [Eq. (6)]. The last row specifies the atomic configuration used to calculate ρ_s and ρ_d.

	Cu	Ag	Au	Ni	Pd	Pt
Z_0	11.0	11.0	11.0	10.0	10.0	10.0
α	1.7227	2.1395	1.4475	1.8633	1.2950	1.2663
β	0.1609	1.3529	0.1269	0.8957	0.0595	0.1305
ν	2	2	2	1	1	1
n_s	1.000	1.6760	1.0809	1.5166	0.8478	1.0571
Atomic configuration	$3d^{10}4s^1$	$4d^95s^2$	$5d^{10}6s^1$	$3d^84s^2$	$4d^95s^1$	$5d^96s^1$

TABLE II. Pure metal properties used to determine the functions: equilibrium lattice constants, sublimation energy, bulk modulus, elastic constants, and vacancy-formation energy. Where two numbers are given, the top number is the value calculated with these functions and the lower number is the experimental value.

	Cu	Ag	Au	Ni	Pd	Pt
a_0 (Å)[a]	3.615	4.09	4.08	3.52	3.89	3.92
E_{sub} (eV)[b]	3.54	2.85	3.93	4.45	3.91	5.77
B (ergs/cm^3)[c]	1.38	1.04	1.67	1.804	1.95	2.83
C_{11} (ergs/cm^3)[c]	1.67	1.29	1.83	2.33	2.18	3.03
	1.70	1.24	1.86	2.465	2.341	3.47
C_{12} (ergs/cm^3)[c]	1.24	0.91	1.59	1.54	1.84	2.73
	1.225	0.934	1.57	1.473	1.76	2.51
C_{44} (ergs/cm^3)[c]	0.76	0.57	0.45	1.28	0.65	0.68
	0.758	0.461	0.42	1.247	0.712	0.765
E_v^f (eV)	1.28	0.97	1.03	1.63	1.44	1.68
	1.3[d]	1.1[d]	0.9[d]	1.6[e]	1.4[f]	1.5[d]

[a]Reference 17.
[b]Reference 18.
[c]Reference 19.
[d]Reference 20.
[e]Reference 21.
[f]Estimated from melting point, see Ref. 22.

conditions (vacancy-formation energy and two conditions from the elastic constants, because the bulk modulus is already determined.) In addition, the mixing enthalpies provide 22 conditions. (Although there are 30 possible mixing enthalpies, experimental data are not available in eight cases.) Thus there are a total of 40 conditions used here to fit these 17 parameters.

The parameters derived from the fit to define the pair interactions and electron density are given in Table I. The properties used in the fitting process are listed in Table II. The resulting functions are shown in Figs. 1 and 2. Note that the effective charges $Z(R)$ tend to group in pairs of similar curves for the elements on the same row of the Periodic Table. The embedding energies also show systematic trends with the functions becoming larger in magnitude as one moves down each column of the Periodic Table.

The calculated values for the elastic constants and vacancy-formation energy of the pure materials are compared with the experimental values to which they were fitted in Table II. The agreement is generally good, though in some cases the difference between the predicted and experimental elastic constants remain as large as 20%. The vacancy-formation energies agree well with the experimental estimates. The typical difference is about 0.1 eV and in no case is larger than 0.2 eV.

The heats of solution calculated from these functions are compared in Table III with the experimental values to which they were fitted. The experimental values are obtained from the composition derivatives of the enthalpy[23]

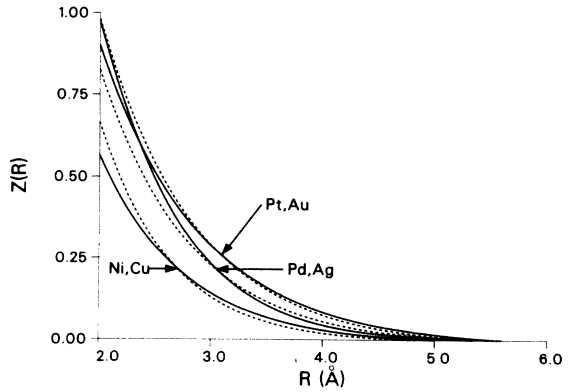

FIG. 1. The effective charge $Z(R)$ used to define the pair interaction [see Eq. (3)] for Cu, Ag, and Au (solid lines) and for Ni, Pd, and Pt (dashed lines). Z is in units of electron charge and R is in Å.

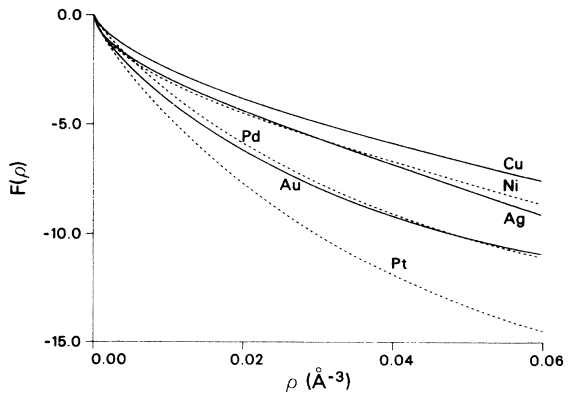

FIG. 2. The embedding functions $F(\rho)$ as a function of background electron density for Cu, Ag, and Au (solid lines) and for Ni, Pd, and Pt (dashed lines). The embedding energy is in eV and the electron densities in Å^{-3}.

TABLE III. Alloy heats of solution for single substitutional impurities used to define the functions. The top number is the value calculated with these functions and the lower number is the experimental energy from Ref. 23. The energies are in eV.

	Host					
	Cu	Ag	Au	Ni	Pd	Pt
Cu		0.18	−0.12	0.06	−0.33	−0.38
		0.25	−0.13	0.11	−0.39	−0.30
Ag	0.11		−0.11	0.42	−0.36	−0.18
	0.39		−0.16		−0.11	
Au	−0.18	−0.11		0.30	−0.15	0.07
	−0.19	−0.19		0.28	−0.20	
Ni	0.04	0.38	0.08		−0.15	−0.25
	0.03		0.22		−0.09	−0.33
Pd	−0.34	−0.24	−0.12	0.07		0.03
	−0.44	−0.29	−0.36	0.06		
Pt	−0.54	−0.07	0.09	−0.28	0.04	
	−0.53			−0.28		

evaluated at the two extremes of the composition range for each alloy pair. The available thermodynamic data are for high temperatures, typically around 1000 K. There has been no attempt here to extrapolate these values to zero temperature, in effect assuming that the finite-temperature effects on the excess enthalpy is zero.

The agreement between the calculated and experimental heats of solution in Table III is generally good, in most cases within 0.1 eV. The largest discrepancies are found for Cu-Ag, Pd-Ag, and Pd-Au. For four of the alloy pairs, detailed thermodynamic data are not available. The resulting heats of solution calculated here are then predictions. In all cases, though, the values obtained here are consistent with the phase diagrams of the alloys. The Ni-Ag system is immiscible up to the melting point.[24] This is consistent with the large positive heats of solution found here. For the Pt-Au system, there is a miscibility gap over a large part of the composition range.[24] This suggests positive heats of solution as found here. The Pd-Pt system forms a continuous series of solid solutions at high temperatures, though there is evidence that there is a miscibility gap near 1050 K.[25] This suggests that the heats of solution should be small but positive. The Pt-Ag system forms a variety of ordered phases.[24] The formation of ordered phases suggests that the Pt-Ag interaction is attractive relative to the Pt-Pt and Ag-Ag interactions. This, in turn, suggests that the heat of solution should be negative as found here.

III. PROPERTIES OF BULK METALS

There is nothing in the fitting procedure used here that insures that the fcc structure will emerge as the most energetically stable structure predicted by these functions. Accordingly, the energy of the bcc and hcp phases of all six metals have been computed. In computing these energies, the lattice constants and c/a ratio of the hcp structure were both varied to obtain the minimum energy for each of these phases. In all cases, the fcc structure was found to be energetically favored over the hcp and bcc structures. The energy differences between these structures was found to be quite small. The energy of the bcc phases is 0.02—0.05 eV above the fcc structures, while the energy of the hcp structures is 0.003—0.01 eV higher than the fcc phases. The c/a ratio of the minimum energy hcp structures is calculated to be within 0.01 of the ideal value $c/a = 1.633$ for all of these metals.

As a further test of these functions, the formation volume and migration energy of vacancies and the formation energy, formation volume, and migration energy of divacancies and self-interstials have been determined. The calculations are performed with a computational cell of about 500 atoms with periodic boundary conditions. (Calculations with more atoms yield the same results to within less than 0.005 eV.) In all cases, the defect energy is minimized with respect to the atomic coordinates of all the atoms in the computational cell. In addition, the energy is minimized with respect to the dimensions of the periodic cell. The change in volume of the computational cell then gives the formation volumes of the vacancies and self-interstitials.

The predictions of the point-defect calculations are presented in Table IV along with experimental estimates, where available. (The vacancy-formation energies are presented in Table II since that value was used in the fitting.) The vacancy migration energies calculated for Cu, Ag, and Au are in good accord with the experimental estimates. For Ni and Pt, the agreement is poorer with the calculated migration energies smaller than the experimentally determined values. This may reflect a deficiency in the functional form of the effective charge chosen for these metals. The migration energy depends on interactions at shorter range than the interactions entering the elastic constants and vacancy-formation energy. Vacancy-formation volumes follow the trends of the available data.

For divacancies, the binding energy is reported rather than the formation energy. The divacancy binding energy

TABLE IV. Calculated point-defect properties: vacancy migration energy E_v^m, vacancy-formation volume ΔV_v^f, divacancy binding energy E_{2v}^b, divacancy migration energy E_{2v}^m, self-interstitial formation energy E_{SI}^f, self-interstitial formation volume ΔV_{SI}^f, and self-interstitial migration energy E_{SI}^m. Ω is the equilibrium atomic volume. The upper values are the theoretical results and the lower values are experimental values where available.

	Cu	Ag	Au	Ni	Pd	Pt
E_v^m (eV)	0.72	0.83	0.71	1.08	0.82	0.85
	0.71[a]	0.66[a]	0.83[a]	1.3[b]		1.43[a]
$\Delta V_v^f/\Omega$	−0.26	−0.15	−0.39	−0.10	−0.34	−0.45
	−0.22[c]	−0.06[d]	−0.55[d]			
E_{2v}^b (eV)	0.27	0.22	0.22	0.40	0.34	0.45
	0.12[e]	0.38[f]	0.2−0.6[a]	0.33[g]		0.1−0.2[a]
E_{2v}^m (eV)	0.38	0.56	0.50	0.66	0.48	0.57
	0.71[f]	0.57[a]	0.70[a]	0.83[g]		1.1[a]
E_{SI}^f (eV)	2.76	3.92	2.46	5.05	3.42	3.51
$\Delta V_{SI}^f/\Omega$	1.74	2.05	1.47	2.11	1.52	1.40
	1.45[c]					
E_{SI}^m (eV)	0.09	0.09	0.06	0.14	0.08	0.07
	0.12[h]			0.14[h]		0.063[h]

[a]Reference 20.
[b]Reference 21.
[c]Reference 26.
[d]Reference 27.
[e]Reference 28.
[f]Reference 29.
[g]Reference 30.
[h]Reference 31.

is the difference between the energy of two first-neighbor vacancies and two well-separated vacancies. A positive value indicates an attraction between the vacancies. The calculations are again in good agreement with the experimental values, with the exception of Pt, for which the calculated binding is larger than the experimental estimates. In all cases, the formation volume of the divacancy was found to be within 0.03 atomic volumes of twice the formation volume of two monovacancies. The migration of divacancies proceeds by the motion of an atom in a lattice site adjacent to both of the vacancy sites into one of the vacancy sites. The barrier for this motion is calculated to be between 0.4 and 0.7 eV. This agrees well with the estimates from radiation-damage experiments for Ag and Au. The experimental values for divacancy migration energies in Pt is significantly higher than the values obtained here, though. This is probably related to the low migration energy calculated for the monovacancy in Pt.

The calculated lowest-energy configuration for self-interstitials is the [100] dumbbell configuration for all of these metals. In this configuration the interstitial atom and a lattice atom form a symmetric pair centered on a lattice site with the axis of the dumbbell along the [100] crystal direction. This agrees with the experimental conclusions about self-interstitial structure based on x-ray scattering analysis.[26] For all cases the energetically next best orientation for the self-interstial dumbbell is along the [110] direction. The formation energy of self-interstitials is computed to be large ranging from 2.5 to 5.0 eV. The formation volume is also computed to be large. The only experimental data on the formation volume is for Cu where the experimental result is in reasonable agreement with our calculations. The migration energy for self-interstitials is computed to be on the order of 0.1 eV. These values agree well with the estimates from radiation-damage experiments for Cu, Ni, and Pt.

IV. PURE METAL SURFACES

The present functions have been used to calculate the surface energy and geometry of the low-index faces, (100), (110), and (111). In all cases, the relaxation from the bulk-terminated geometries was allowed to occur, but no effort was made in these calculations to search for energetically favored reconstructions. The EAM is a good tool for the investigation of reconstruction, though. In particular, Daw has shown that these functions predict that the (1×2) missing-row reconstruction of the Pt(110) surface is lower in energy than the unreconstructed surface.[10] This result agrees with the experimental observation of a (1×2) reconstruction of that surface.[32] A systematic study of the possible reconstructions of the clean surfaces of these metals is in progress.

The surface energies obtained for the low-index faces of these six metals are presented in Table V. The surface energies are calculated by comparing the energy of a periodic slab of atoms to the energy of the same number of atoms in the bulk material. For all cases, the close-packed (111) face has the lowest energy, followed by the (100) and (110) faces. This table also contains the estimates, due to Tyson and Miller,[33] of the surface energy based on liquid-metal surface energies. The calculated surface energies are consistently lower than these estimates. This difference may be due, in part, to the presence of less energetically favorable faces and defects on the average sur-

TABLE V. Calculated surface energies of the low-index faces and the experimental average surface energy from Ref. 33 in units of ergs/cm^2.

	Cu	Ag	Au	Ni	Pd	Pt
(111)	1170	620	790	1450	1220	1440
(100)	1280	705	918	1580	1370	1650
(110)	1400	770	980	1730	1490	1750
Experimental (average face)	1790	1240	1500	2380	2000	2490

face for which these estimates are intended. In addition, there is significant uncertainty in the estimates of the surface energy, as evidenced by the wide range of values obtained by different researchers.[34] The trends from element to element in the surface energies calculated here do agree with the trends found also in the experimental data.

The change in the interlayer spacings, Δz, computed for the relaxed surface geometries relative to the spacings for the truncated bulk geometries are presented in Table VI. Note that all the top-layer spacings show a small contraction. Further, the rougher (110) surfaces show larger relaxations than do the smoother (100) and (111) faces. Both of these general features agree with the trends found in the experimental data.[35] There have been many experiments performed to determine these relaxations using low-energy electron diffraction and ion scattering. Below, we compare our calculated values for the surface relaxations with the recent experimental results of which the authors are aware.

The relaxations of the (100) and (111) faces of Cu have been found experimentally to be fairly small, about -0.02 Å.[36] This agrees well with our results. The first-layer contractions determined experimentally for the (110) surface of Cu (Ref. 37) range from -0.07 to -0.11 Å, in reasonable agreement with our values. The second-layer spacing for this surface is experimentally found to increase by 0.03—0.04 Å. While our results do show a small second-layer expansion, it is smaller by about an order of magnitude. The same general conclusion holds for Ag. There, the experimental contraction[37] of the (111) face was found to be <0.05 Å, consistent with our calculations. The experimental determinations of the change in the first-layer spacing of the (110) face range from -0.08 to -0.11 Å.[37] The second-layer spacing is found to increase by 0.03—0.06 Å. Detailed comparison of our results for Au are unfortunately not possible since both the (100) and (110) surfaces reconstruct and the authors are not aware of any recent measurements of the relaxation on the (111) face. The relaxations for the Ni(100) and Ni(111) have been measured to be very small, <0.02 Å.[5] This is in agreement with our results. The (110) relaxations were measured to be somewhat larger than our results, namely -0.06 or -0.10 Å. No results were found for the relaxation of the clean surfaces of Pd and comparison with the (100) and (110) faces of Pt is not possible since they undergo reconstruction. In general, the trends found in our results for the surface relaxations agree well with experiment but the magnitude of the effects, especially for second-layer relaxations, may be underestimated by the present functions.

V. ALLOY SURFACES

The segregation of alloying elements at inhomogeneities such as a surface is of great importance. In order to test the ability of these functions to correctly predict segregation, the zero-temperature energetics of an impurity atom near a (100) surface have been computed. Table VII presents the energy of a substitutional impurity atom in either the first or second atomic layer of a (100) face of a pure metal slab, computed relative to the energy of that substitutional impurity in the bulk. A negative value of this energy thus implies that the impurity in question will be enriched in that atomic layer. A positive value implies depletion of that element. Of course, these energies are computed in the dilute limit and can change substantially if there is a significant concentration of the impurity near the surface. The utility of these numbers is that they indicate the segregating species and suggest the magnitude of the segregation.

The segregating species is known experimentally for 18 of the cases examined here.[38—40] In all of these cases, the calculations predict that the experimentally observed segregating species will be enriched in either the first or

TABLE VI. Surface relaxation of the top-layer spacing Δz_{12}, and of the second layer spacing Δz_{23}, for the low-index faces. These values are calculated for unreconstructed geometries. Distances are expressed in Å.

		Cu	Ag	Au	Ni	Pd	Pt
(100)	Δz_{12}	−0.026	−0.038	−0.128	−0.004	−0.085	−0.135
	Δz_{23}	−0.006	−0.001	0.011	−0.002	−0.001	0.012
(110)	Δz_{12}	−0.063	−0.074	−0.220	−0.029	−0.155	−0.244
	Δz_{23}	0.003	0.005	0.031	0.001	0.016	0.036
(111)	Δz_{12}	−0.029	−0.031	−0.100	−0.011	−0.072	−0.109
	Δz_{23}	−0.001	0.001	0.015	0.000	0.006	0.017

TABLE VII. The energy of a single impurity in the first and second atomic layers of a (100) surface relative to the energy of the impurity in the bulk of the host material. The energies are given in eV. The first line is the energy in the first atomic layer and the second line is the energy in the second atomic layer.

	Host					
	Cu	Ag	Au	Ni	Pd	Pt
Cu		0.10	0.15	−0.18	0.03	−0.04
		−0.01	−0.07	0.02	−0.12	−0.09
Ag	−0.46		−0.07	−0.75	−0.25	−0.44
	−0.04		−0.03	−0.03	−0.15	−0.06
Au	−0.40	0.11		−0.94	−0.18	−0.49
	−0.01	0.01		−0.03	−0.08	0.04
Ni	0.11	0.11	0.15		0.02	−0.01
	−0.03	−0.03	−0.13		−0.19	−0.20
Pd	−0.13	0.24	0.21	−0.62		−0.23
	0.04	0.02	0.04	0.02		0.12
Pt	0.15	0.42	0.38	−0.32	0.22	
	0.01	−0.01	−0.05	0.00	−0.10	

second atomic layer. There are two interesting features in these results. First, in many cases the sign of the segregation energy differs for the two planes. This suggest that the composition profile may oscillate in these cases. Such behavior was found in the study of the Ni-Cu system using the EAM,[11] as well as in field-ion-microscopy studies of the composition profile of that system.[41] Second, for Cu or Ni in Pd or Pt hosts, the segregation energy is larger for the second layer than for the first. This suggests rather interesting composition profiles for these cases.

VI. SUMMARY

This paper presents a set of embedding energies, pair interactions, and atomic densities to be used with the EAM to describe pure metals and alloys containing Cu, Ag, Au, Ni, Pd, or Pt. These functions were determined by assuming simple functional forms which were adjusted to yield the bulk sublimation energy, elastic constants, vacancy-formation energies, and binary alloy heats of solution. We have endeavored here to use the simplest parametrized forms possible with the fewest number of parameters. The use of more flexible functional forms may produce functions that more accurately describe a given metal or alloy. The simple functional forms used here with the relatively small number of adjustable parameters were chosen to make the fit to a large number of alloy combinations computationally feasible. Thus, better fits may be possible for describing a smaller number of elements. Further, more experimental data could be used in the fitting process to determine the functions more reliably.

The validity of these functions has then been tested by applying them to a wide variety of bulk and surface properties of both the pure metals and the alloys. The calculated properties for the pure metals include point-defect properties and surface energies and geometries. The calculated alloy properties are the segregation energies of substitutional impurities to the (100) surface. The agreement between the calculations and the available experiment data is generally quite good, especially considering the wide range of properties determined. In addition, some interesting predictions have been made about the details of surface segregation.

ACKNOWLEDGMENTS

The technical assistance of Ms. Julie Edwards in performing these calculations is greatly appreciated. This work was supported by the United States Department of Energy.

[1]R. A. Johnson and W. D. Wilson, in *Interatomic Potentials and Simulation of Lattice Defects,* edited by P. C. Gehlen, J. R. Beeler, and R. I. Jaffee (Plenum, New York, 1971).
[2]R. A. Johnson, J. Phys. F **3**, 295 (1973).
[3]M. I. Baskes and C. F. Melius, Phys. Rev. B **20**, 3197 (1979).
[4]M. S. Daw and M. I. Baskes, Phys. Rev. Lett. **50**, 1285 (1983).
[5]M. S. Daw and M. I. Baskes, Phys. Rev. B **29**, 6443 (1984).
[6]R. A. Johnson, Phys. Rev. B **6**, 2094 (1972).
[7]M. S. Daw and R. L. Hatcher, Solid State Commun. **56**, 697 (1985).
[8]S. M. Foiles, Phys. Rev. B **32**, 3409 (1985).
[9]M. S. Daw, M. I. Baskes, and W. G. Wolfer, in *Proceedings of the Special Symposium on Modelling Environmental Effects on Crack Initiation and Propagation, Toronto, 1985,* (AIME,

New York, in press).
[10]M. S. Daw, Surf. Sci. Lett. **166**, L161 (1986).
[11]S. M. Foiles, Phys. Rev. B **32**, 7685 (1985).
[12]S. M. Foiles and M. S. Daw, J. Vac. Sci. Technol. A **3**, 1565 (1985).
[13]M. S. Daw (unpublished).
[14]E. Clementi and C. Roetti, At. Data Nucl. Data Tables **14**, 177 (1974).
[15]A. D. McLean and R. S. McLean, At. Data Nucl. Data Tables **26**, 197 (1981).
[16]J. H. Rose, J. R. Smith, F. Guinea, and J. Ferrante, Phys. Rev. B **29**, 2963 (1984).
[17]N. W. Ashcroft and N. D. Mermin, *Solid State Physics* (Holt, Rinehart and Winston, New York, 1976).
[18]*Metal Reference Book*, 5th ed., edited by C. J. Smith (Butterworths, London, 1976), p. 186.
[19]G. Simmons and H. Wang, *Single Crystal Elastic Constants and Calculated Aggregate Properties: A Handbook* (MIT Press, Cambridge, 1971).
[20]R. W. Balluffi, J. Nucl. Mater. **69&70**, 240 (1978).
[21]W. Wycisk and M. Feller-Kniepmeier, J. Nucl. Mater. **69&70**, 616 (1978).
[22]Y. A. Kraftmakher and P. G. Strelkov, in *Vacancies and Interstitials in Metals*, edited by A. Seeger, D. Schumacher, W. Schilling, and J. Diehl (North-Holland, Amsterdam, 1970), p. 59.
[23]R. Hultgren, P. D. Desai, D. T. Hawkins, M. Gleiser, and K. K. Kelley, *Selected Values of the Thermodynamic Properties of Binary Alloys* (American Society for Metals, Metals Park, OH, 1973).
[24]M. Hansen, *Constitution of Binary Alloys* (McGraw-Hill, New York, 1958).
[25]F. A. Shunk, *Constitution of Binary Alloys, Second Supplement* (McGraw-Hill, New York, 1969).
[26]P. Ehrhart, J. Nucl. Mater. **69&70**, 200 (1978).
[27]P. Ehrhart, in *Vacancies and Interstitials in Metals*, Ref. 22, p. 363.
[28]A. Seeger and H. Mehrer, in *Vacancies and Interstitials in Metals*, Ref. 22, p. 1.
[29]J. S. Koehler, in *Vacancies and Interstitials in Metals*, Ref. 22, p. 169.
[30]H. Kronmuller, in *Vacancies and Interstitials in Metals*, Ref. 22, p. 183.
[31]F. W. Young, Jr., J. Nucl. Mater. **69&70**, 310 (1978).
[32]D. W. Blakely and G. A. Somorjai, Surf. Sci. **65**, 419 (1977).
[33]W. R. Tyson and W. A. Miller, Surf. Sci. **62**, 267 (1977).
[34]W. R. Tyson, Can. Met. Quart, **14**, 307 (1975).
[35]M. A. Van Hove, in *The Nature of the Surface Chemical Bond*, edited by T. N. Rhodin and G. Ertl (North-Holland, Amsterdam, 1979).
[36]S. A. Lindgren, L. Wallden, J. Rundgren, and P. Westrin, Phys. Rev. B **29**, 576 (1984).
[37]Y. Kuk and L. C. Feldman, Phys. Rev. B **30**, 5811 (1984), and references therein.
[38]J. C. Hamilton, Phys. Rev. Lett. **42**, 989 (1979).
[39]P. Wynblatt and R. C. Ku, in *Interfacial Segregation*, edited by W. C. Johnson and J. M. Blakely (American Society for Metals, Metals Park, OH, 1979).
[40]A. D. Van Langeveld, H. A. C. M. Hendrickx, and B. E. Nieuwenhuys, Thin Solid Films **109**, 179 (1983).
[41]Y. S. Ng, T. T. Tsong, and S. B. McLane, Jr., Phys. Rev. Lett. **42**, 588 (1979).